International Journal of Mathematics Trends and Technology
ISSN: 2231 - 5373/doi:10.14445/22315373/IJMTT-V68I1P512
Volume 68 Issue 1, 101-114, January, 2022

Review Article

Fast Solution for the Nonlinear Schrodinger Equation in Optical Fibers by the Reduced Basis Method

Pa Mahmud Kah[#1], Phineas Roy Kiogora[*2], Kennedy Awuor[#3], Churchill Saoke[*4]

[#1] *Mathematics Department, Pan African University, Institute for Basic Sciences Technology and Innovation, Kenya*

[*2,*4] *Mathematics Department, Jomo Kenyatta University of Agriculture and Technology, Kenya*

[#3] *Mathematics and Acturial Science Department, Kenyatta University, Kenya*

Abstract - Nonlinear Schrödinger Equation (NLSE) is a universal nonlinear model which portrays several physical nonlinear systems. Among other natural phenomena the one-dimensional NLSE models, light pulses in optical fibers and the dilut-gas Bose-Einstein condensates (BEC) in quasi one-dimensional regime. In this research application of the NLSE in optical fibers is emphasized. However, the numerical solution for the NLSE encounters several computational challenges such as cost and time. Therefore, we employ the Reduced Basis Method (RBM) which significantly reduced these computational cost and time and thus accelerate numerical simulations. We came up with a faster and cheaper numerical solution of the NLSE in fiber optics and our results presented can be applied in communication systems.

Keywords - Dispersion, Fiber Optics, NLSE, Nonlinearity, RBM.

I. INTRODUCTION

Nonlinear optical fiber is a division of optics that explores the nonlinear optical phenomena that takes place inside optical fibers. When fiber losses fell below $20dB/Km$ in 1970, optical fiber communications became financially viable, allowing the widespread adoption of optical fibers for communication purposes. Rayleigh scattering was the primary constraint on performance in the $1.55\mu m$ wavelength range until 1979, when manufacturing technology reduced the loss level to $0.2dB/Km$ [6] . The development of high-capacity fiber optic communication networks, as well as significant breakthroughs in light wave technology, ensured that fiber optics remained a dominant technology throughout the 1990s. We used optical amplifiers to neutralize the fiber loss in these systems by amplifying the transmitted signals at regular intervals. Therefore, long distances can collect nonlinear effects that are present in the fiber, resulting in an effective interaction length of thousands of kilometres. Schrodinger equation governs the wave function in a quantum-mechanical system, a fundamental

principle of quantum mechanics, its discovery marked a turning point in the development of the discipline. Erwin Schrodinger (1887-1961) proposed the equation in 1925 and it was published in 1926. Thus, the name Schrodinger Equation. This landmark established the foundation for his Nobel Prize in Physics in 1933.

The NLSE, is a classical field equation which is applicable to light propagation in nonlinear fiber optics, Bose–Einstein condensates and to planar waveguides. Light has been our primary means of communication for thousands of years. A single piece of information has been communicated by civilizations using mirrors, fire beacons, and smoke signals (such as victory in a war). Campfires were utilised to illuminate our path back to camp at night and to scare away any dangerous wildlife from our campsite. In order to warn of an impending attack, signal bonfires were lighted on nearby hillsides. In this high-tech age of satellite communications, ships still carry a bright lamp as a safety precaution [10].

Light was first used to broadcast speech in 1880, just four years after Alexander Graham Bell invented the telephone. He termed his gadget *photo-phone*. It consisted a tube with a flexible mirror attached to the end. His voice shook the mirror as he spoke into the tube, as a result, a photocell placed around $200m$ away recognised the modulated light. While the method was far from flawless, it enabled the speaker to be understood within a short distance [10]. With the introduction of telegraphy in the 1830s, Electricity superseded light as a medium of communication. The use of intermediate relay stations (up to $1000Km$) enabled long-distance communication, which was noteworthy at the time. When the telephone was invented in 1876, it radically changed the electrical communication system. As telephone networks grew across the globe during the twentieth century, developments were accelerated in its design. By changing from wire pairs to coaxial cables, the system's capacity was considerably increased. A coaxial cable of $3MHz$ with the capability of transmitting one television channel or 300 voice channels was installed in 1940. In such systems, the frequency dependent cable losses limits the bandwidth, which increases fast over $10MHz$. As a result of this constraint, microwave communication systems were developed, which carry data via an electromagnetic carrier wave at a frequency interval of $1 - 10GHz$ [8]. The first microwave system was operational in 1948, with a carrier frequency of $4 - GHz$. Since then, substantial breakthroughs have been achieved in the building of coaxial and microwave systems, which can today function at bit rates of up to $100Mb/s$. As of 1975, the most current coaxial system could carry data at a rate of $274Mb/s$. The narrow repeater spacing (1km) in such coaxial lines is a big disadvantage, rendering the system very costly to operate. As a result, fiber optics was proposed as the ideal solution for communication networks [10].

According to [3], the expansion of fiber optics was encouraged by considerable improvements in light wave technology during the 1990s, especially the introduction of high-amplitude optical fiber communication systems, the periodic amplification of transmitted signals by optical amplifiers compensates the continuing fiber loss. Thus, the nonlinear properties of the fiber can accumulate over extended distances, resulting in an effective interaction length of thousands of miles. An optical fiber's core is enclosed in a cladding with a refractive index slightly lower than the core.

A dimensionless parameter characterize The guiding principless of an optical fiber defined as $V = a(\omega/c)(n_1^2 - n_2^2)^{1/2}$ where number of modes the fiber can accomodate is determined by V, a represents core radius, ω represents light frequency and n_1, n_2 represents the core and cladding refractive indices, respectively. Fibers were $V < 2.405$ only accomodate single modes, thus the term *single-mode fibers* [2]. This research focuses on light propagation in single-mode fibers by the nonlinear Schrodinger equation in the presence of dispersion and nonlinearity. While evolutionary partial differential equations (PDEs) often employ a 'space' variable as the evolution variable, our NLSE uses the longitudinal coordinate of the fiber as the evolution variable. The Schrodinger equation, which is nonlinear in nature, regulates narrowband signal propagation in a single-mode fiber. Thus, adopting the signal received as boundary condition (BC), an initial value problem (IVP) can be utilised to recover the broadcast signal in the absence of noise. In practice, an analog-to-digital converter is employed to convert the signal received to digital form, from which we can solve the IVP through a digital signal processing (DSP). We called such a technique digital back propagation (DBP) [5].

Since the NLSE cannot be solved analytically, numerical procedures are used. Numerical solutions to PDE-constrained optimization challenges are often computationally demanding. Substantial computational savings becomes possible using the reduced basis method (RBM) [7]. Numerous SSFM and S-SSFM algorithms have been presented to ease the computational pressures associated with NLSE numerical solutions, but their accuracy, processing time, and cost can potentially be improved. Thus, our purpose is to lower the computing complexity of the NLSE in fiber optics by implementing the RBM, to acquire a more accurate solution and requires less computational time and money to implement than the other techniques.

II. FIBER CHARACTERISTICS

An optical fiber is constructed of pure glass (silica). It operates as a waveguide between the two fiber ends, conveying light. Fiber-optic communications, which are capable of transmitting across higher bandwidths and greater distances, makes substantial use of fiber optics, which are prevalent in this technology. Because fibers have less signal loss and electromagnetic interference than metal lines, they are used in place of metal wires [6].

The optically transparent core is surrounded by a lower refractive index cladding material, which is common in optical fiber. When a light beam contacts a medium boundary at an angle where the critical angle relative to the surface normal is smaller than that angle, the light remains in the core, and such a phenomenon is called Total internal reflection. Light cannot travel through a boundary if on the other side its refractive index is lower and the critical angle is smaller than the incidence angle. As a result, the fiber serves as a waveguide. Fibers with low loss are made of pure silica glass, which is formed by fusing $SiO2$ molecules together. The selective application of dopants during the core and cladding manufacturing processes results in a refractive-index discrepancy. Fluorine and Boron are suitable for cladding, since they diminish silica's refractive index, making them acceptable for the core of an optical fiber [10].

III. THE REDUCED BASIS METHOD

The RBM provides computational speedup to parametrized PDE solutions without compromising the accuracy of its approximation. The RBM is part of a large category of model order reduction methods, whose main goal is reducing the computational burden of a particular problem while preserving relevant properties like stability and accuracy of the system [14].

The RBM is a mathematical and computational scheme for parametric model order reduction of PDEs. We enter the parameters as coefficients in a parametrized PDE or via coefficient functions that defines the systems physical properties or the systems connection with the environment. The key observation of the RBM is that the parameter dependence induced a typically low-dimensional manifold where the answer of this equation dwell. The PDE's solution smoothly varies with the parameters, when the manifold is smooth. The reconstruction of a good approximation of the solution associated with any parameter value should be possible with only little knowledge of the manifold [9].

IV. DISCRETIZATION OF THE NLSE

The NLSE governing optical pulse propagation inside single-mode fiber [1] is presented as follows:

$$i\frac{\partial\psi(z,t)}{\partial t} - \frac{\beta_2}{2}\frac{\partial^2\psi(z,t)}{\partial z^2} + \gamma|\psi(z,t)|^2\psi(z,t) = 0 \tag{1}$$

where $\psi(z,t)$ is the slowly varying amplitude of the pulse envelope, $(\beta_2 \in \mathbb{R}\backslash\{0\})$ is the Chromatic Dispersion (CD), $(\gamma > 0)$ is the nonlinear parameter and $i = \sqrt{-1}$.
given the initial condition

$$\psi(z,0) = g(z) \tag{2}$$

and the boundary condition

$$\frac{\partial\psi}{\partial z}(z,t) = 0, at z = z_L, z_R, \tag{3}$$

We are using the Crank–Nicolson method to solve the NLSE (equation 1). To enforce such a method, we propose that the complex function $\psi(z,t)$ takes the form below:

$$\psi(z,t) = u(z,t) + i\dot{v}(z,t) \tag{4}$$

where $v(z,t)$ and $u(z,t)$ are real functions, therefore, the BC (3) takes the form:

$$\frac{\partial u}{\partial z}(z,t) = \frac{\partial v}{\partial z}(z,t) = 0, \text{ when } z = z_L, z_R \tag{5}$$

Substituting Equation (4) into (1) and writing the real and imaginary parts of the subsequent equation separately we have:

$$\frac{\partial u}{\partial t} - \frac{\beta_2}{2}\frac{\partial^2 v}{\partial z^2} + \gamma\left(u^2 + v^2\right)v = 0 \tag{6}$$

$$\frac{\partial v}{\partial t}+\frac{\beta_2}{2}\frac{\partial^2 u}{\partial z^2}-\gamma\left(u^2+v^2\right)u=0 \tag{7}$$

we can now write Equations (6) and (7) in the following form:

$$\frac{\partial}{\partial t}\begin{bmatrix} u \\ v \end{bmatrix}-\frac{\beta_2}{2}\begin{pmatrix} 0 & 1 \\ -1 & 0 \end{pmatrix}\frac{\partial^2}{\partial z^2}\begin{bmatrix} u \\ v \end{bmatrix}+\gamma\begin{pmatrix} 0 & u^2+v^2 \\ -\left(u^2+v^2\right) & 0 \end{pmatrix}\begin{bmatrix} u \\ v \end{bmatrix}=\begin{bmatrix} 0 \\ 0 \end{bmatrix} \tag{8}$$

Let

$$\psi=\begin{bmatrix} u \\ v \end{bmatrix}, A=\begin{pmatrix} 0 & 1 \\ -1 & 0 \end{pmatrix}, G(\psi)=\begin{pmatrix} 0 & u^2+v^2 \\ -\left(u^2+v^2\right) & 0 \end{pmatrix} \tag{9}$$

Therefore Equations (6) and (7) takes the following form:

$$\frac{\partial \psi}{\partial t}-\frac{\beta_2}{2}A\frac{\partial^2 \psi}{\partial z^2}+\gamma G(\psi)\psi=0 \tag{10}$$

Space Discretization

To generate a numerical method that can solve Equation (10), we assume that the region $R=[z_L<z<z_R]\times[t>0]$ and its boundary ∂R comprising the coordinates $z=z_L, z=z_R$ and the axis $t=0$ is covered with mesh of points that is rectangular in nature and has the coordinates below:

$$z=z_m=z_L+(m-1)h \tag{11}$$

$$h=\frac{z_R-z_L}{N-1}, m=1,2,\ldots,N \tag{12}$$

where h is the length of any two consecutive points and N is the number of points in the grid. Approximate the exact solutions $u(z_m,t)=u_m$ and $v(z_m,t)=v_m$, by the approximation solutions $U(z_m,t)=U_m$ and $V(z_m,t)=V_m$, respectively. Also, use the central difference formula below to approximate the second derivative in Equation (10).

$$\left[\frac{\partial^2 u(z,t)}{\partial z^2}\right]_{(z=z_m,t)}=\frac{1}{h^2}\left[\delta_z^2 u\right]_{(z=z_m,t)}+O\left(h^2\right) \tag{13}$$

where

$$\left[\delta_z^2 u\right]_{(z=z_m,t)}=v\left(z_m+h,t\right)-2u\left(z_m,t\right)+u\left(z_m-h,t\right) \tag{14}$$

which can be written briefly as follows:

$$\frac{\partial^2 u_m}{\partial z^2}=\frac{1}{h^2}\left(u_{m+1}-2u_m+u_{m-1}\right)+O\left(h^2\right) \tag{15}$$

Similarly, $v(z,t)$ takes the form:

$$\frac{\partial^2 v_m}{\partial z^2}=\frac{1}{h^2}\left[\delta_z^2 v\right]_{(z=z_n,t)}+O\left(h^2\right)=\frac{1}{h^2}\left(v_{m+1}-2v_m+v_{m-1}\right)+O\left(h^2\right) \tag{16}$$

Substituting Equations (15) and (16) into (6) and (7) gives the following correlations:

$$\dot{U}_m-\frac{\beta_2}{2h^2}\left(V_{m+1}-2V_m+V_{m-1}\right)+\gamma\left(U_m^2+V_m^2\right)V_m=0, \quad m=1,2,\ldots,N \tag{17}$$

$$\dot{V}_m+\frac{\beta_2}{2h^2}\left(U_{m+1}-2U_m+U_{m-1}\right)-\gamma\left(U_m^2+V_m^2\right)U_m=0 \tag{18}$$

which we can write as:

$$\dot{\Psi}_m-\frac{\beta_2}{2h^2}A\delta_z^2\Phi_m+\gamma G\left(\Psi_m\right)\Psi_m=0 \tag{19}$$

where after using the approximate solutions U and V, we drop the error term, 0 is a $2N \times 1$ zero vector, and

$$\Psi = \begin{bmatrix} U \\ V \end{bmatrix} \tag{20}$$

Further, we approximate the BC (3) using the central difference formula:

$$\frac{\partial U_m}{\partial z} = \frac{1}{2h}\left(U_{m+1} - U_{m-1}\right) = 0 \tag{21}$$

$$\frac{\partial V_m}{\partial z} = \frac{1}{2h}\left(V_{m+1} - V_{m-1}\right) = 0, \quad \text{when} \quad m = 1, N \tag{22}$$

where $z_1 = z_L$ and $z_N = z_R$ which imply the following relation:

$$U_0 = U_2, V_0 = V_2, U_{N+1} = U_{N-1}, V_{N+1} = V_{N-1} \tag{23}$$

Using the BC (23), we can write equations (17) and (18) as follows:

$$\Psi + [S + B(\Psi)]\Psi = 0 \tag{24}$$

where

$$\Psi = \left[\Psi_1^T, \Psi_2^T, \cdots, \Psi_N^T\right]^T, \Psi_m = \left[U_m, V_m\right]^T, m = 1, 2, \ldots N \tag{25}$$

S and $B(\Psi)$ are $N \times N$ block tridiagonal matrices in the form below:

$$S = \frac{\beta_2}{2h^2}\begin{pmatrix} 2A & -2A & x & x & \cdots & x \\ -A & 2A & -A & x & \cdots & x \\ x & -A & \cdots & -A & \cdots & \vdots \\ \vdots & \cdots & \cdots & \cdots & \cdots & x \\ x & \cdots & x & -A & 2A & -A \\ x & x & \cdots & x & -2A & 2A \end{pmatrix}, B(\Psi) = \operatorname{diag}\left[B_1\left(\Psi_1\right), B_2\left(\Psi_2\right), \ldots, B_N\left(\Psi_N\right)\right] \tag{26}$$

$$B_m\left(\Psi_m\right) = \begin{pmatrix} 0 & \gamma\left(V_m^2 + W_m^2\right) \\ -\gamma\left(V_m^2 + W_m^2\right) & 0 \end{pmatrix} \tag{27}$$

0 is $2N \times 1$ zero vector and x is 2×2 zero matrix.

Time Discretization

Suppose that Ψ_m^n is the fully discrete approximation to

$\Psi\left(z_m, t_n\right) = U\left(z_m, t_n\right) + iV\left(z_m, t_n\right)$, where

$t_n = nk, n = 0, 1, 2, \ldots$

and k is time increment.

For the integration with respect to time of the system in (24), we use the implicit point rule below

$$\Psi_m^n = \frac{\Psi_m^{n+1} + \Psi_m^n}{2}, m = 1, 2, \ldots N \tag{28}$$

and using the forward difference below for the derivatives in time,

$$(\dot{\Psi})_m^n = \frac{\Psi_m^{n+1} - \Psi_m^n}{k} \tag{29}$$

Ignoring the truncation error $O(k)$. Then, the system in (24) takes the following form:

$$\Psi^{n+1} - \Psi^n + k\left[S + B\left(\frac{\Psi^{n+1} + \Psi^n}{2}\right)\right]\left(\frac{\Psi^{n+1} + \Psi^n}{2}\right) = \mathbf{0} \tag{30}$$

representing a block nonlinear tridiagonal system of $2N$ nonlinear algebraic equations which we can solve by the Newton's method.

Newton's Method

We can write equation (30) as follows:

$$F(\Psi) = 0 \tag{31}$$

where 0 is $2N \times 1$ zero vector and

$$F(\mathbf{\Psi}) = \left[f_1^T, f_2^T, \ldots, f_N^T\right]^T, f_m = \left[(f1)_m, (f2)_m\right]^T, \Psi = \left[\Psi_1^T, \Psi_2^T, \cdots, \Psi_N^T\right]^T, \Psi_m = \left[U_m, V_m\right]^T, m = 1, 2, \ldots, N \tag{32}$$

where $(f1)_m$ and $(f2)_m$ are nonlinear functions.
We can apply Newton's method as:

$$\Psi^{(j+1)} = \Psi^{(j)} - J^{-1}\left(\Psi^{(j)}\right) F\left(\Psi^{(j)}\right), j = 0, 1, 2, \ldots \tag{33}$$

where j is the number of iterations and J is the Jacobian $N \times N$ block tridiagonal matrix as:

$$J(\mathbf{\Psi}) = \begin{pmatrix} A_1 & C_1 & x & \cdots & x \\ B_2 & A_2 & \vdots & \vdots & \vdots \\ x & \vdots & \vdots & \vdots & x \\ \vdots & \vdots & \vdots & \vdots & C_{N-1} \\ x & \cdots & x & B_N & A_N \end{pmatrix} \tag{34}$$

where A, B and C are 2×2 matrices in the form:
$A_i = \begin{pmatrix} \frac{\partial(f1)_i}{\partial U_i} & \frac{\partial(f1)_i}{\partial V_i} \\ \frac{\partial(f2)_i}{\partial U_i} & \frac{\partial(f2)_i}{\partial V_i} \end{pmatrix}, i = 1, 2, \ldots, N, B_i = \begin{pmatrix} \frac{\partial(f1)_i}{\partial U_{i-1}} & \frac{\partial(f1)_i}{\partial V_{i-1}} \\ \frac{\partial(f2)_i}{\partial U_{i-1}} & \frac{\partial(f2)_i}{\partial V_{i-1}} \end{pmatrix}, i = 2, 3, \ldots, N$
$C_i = \begin{pmatrix} \frac{\partial(f1)_i}{\partial U_{i+1}} & \frac{\partial(f1)_i}{\partial V_{i+1}} \\ \frac{\partial(f2)_i}{\partial U_{i+1}} & \frac{\partial(f2)_i}{\partial V_{i+1}} \end{pmatrix}, i = 1, 2, ..., N-1$ we can calculate the system (33) by firstly, introducing the $2N \times 1$ vector y to satisfy the relation below:

$$J\left(\Psi^{(j)}\right) y = F\left(\Psi^{(j)}\right), \quad j = 0, 1 \ldots \tag{35}$$

which we can obtain by using Gauss elimination to solve the system in (35). And secondly by substituting the vector y in the relation below:

$$\Psi^{(j+1)} = \Psi^{(j)} - y \tag{36}$$

to update the initial guess vector $\Psi^{(j)}$. Therefore, we apply (35) and (36) until the relation below is satisfied:

$$\left\|\Psi^{(j+1)} - \Psi^{(j)}\right\|_\infty < tol \tag{37}$$

where *tol* refers to a small value prescribed to measure the errors.

Accuracy and Stability of the Method

A numerical method's order of accuracy means how fast errors decrease in the limit as the step size tends to zero. Studying the accuracy of the Crank–Nicolson method used here, Equations (28) and (29) will be substituted into the system (19) to have

$$\frac{\psi_m^{n+1}-\psi_m^n}{k}-\frac{\beta}{2h^2}A\delta_z^2\left(\frac{\psi_m^{n+1}+\psi_m^n}{2}\right)+\gamma\boldsymbol{g}\left(\frac{\psi_m^{n+1}+\psi_m^n}{2}\right)=\mathbf{0} \tag{38}$$

where

$$G\left(\boldsymbol{\psi}_m\right)\boldsymbol{\psi}_m=\mathbf{g}\left(\boldsymbol{\psi}_m\right) \tag{39}$$

To obtain the expansions below we use Taylor's series expansion of all terms in (38) about ψ_m^n where it is the exact solution vector of the NLSE.

$$\psi_m^{n+1}=\left[\psi+k\frac{\partial\psi}{\partial t}+\frac{k^2}{2!}\frac{\partial^2\psi}{\partial t^2}+O\left(k^3\right)\right]_m^n$$

$$\psi_{m\pm1}^n=\left[\psi\pm h\frac{\partial\psi}{\partial z}+\frac{h^2}{2!}\frac{\partial^2\psi}{\partial z^2}\pm\frac{h^3}{3!}\frac{\delta^3\psi}{\partial z^3}+\frac{h^4}{4!}\frac{\partial^4\psi}{\partial z^4}+O\left(h^5\right)\right]_m^n$$

$$\psi_{m+1}^{n+1}=\sum_{p=0}^{\infty}\frac{1}{p!}\left[h\frac{\partial}{\partial z}+k\frac{\partial}{\partial t}\right]^p\psi_m^n$$

$$\psi_{m-1}^{n+1}=\sum_{p=0}^{\infty}\frac{1}{p!}\left[k\frac{\partial}{\partial t}-h\frac{\partial}{\partial z}\right]^p\psi_m^n$$

where

$$\begin{aligned}\delta_z^2\psi_m^n&=\psi_{m+1}^n-2\psi_m^n+\psi_{m-1}^n\\ \delta_z^2\psi_m^{n+1}&=\psi_{m+1}^{n+1}-2\psi_m^{n+1}+\psi_{m-1}^n\end{aligned} \tag{40}$$

which gives

$$\begin{aligned}\delta_z^2\boldsymbol{\psi}_m^n&=\left[h^2\frac{\partial^2\psi}{\partial z^2}+\frac{1}{12}h^4\frac{\partial^4\psi}{\partial z^4}\right]_m^n+\ldots\\ \delta_z^2\psi_m^{n+1}&=\left[h^2\frac{\partial^2\psi}{\partial z^2}+kh^2\frac{\partial^3\psi}{\partial z^2\partial t}+\frac{k^2h^2}{2}\frac{\partial^4\psi}{\partial z^2\partial t^2}+\frac{k^4}{12}\frac{\partial^4\psi}{\partial t^+}+\frac{h^4}{12}\frac{\partial^4\psi^n}{\partial z^4}\right]_m^n+\ldots\end{aligned} \tag{41}$$

and thus, the following expansions are obtained:

$$\frac{\psi_m^{n+1}-\psi_m^n}{k}=\left[\frac{\partial\psi}{\partial t}+\frac{k}{2}\frac{\partial^2\psi}{\partial t^2}+\frac{k^2}{3!}\frac{\partial^3\psi}{\partial t^3}+O\left(k^3\right)\right]_m^n \tag{42}$$

$$\frac{1}{4h^2}\delta_z^2\left(\boldsymbol{\psi}_m^{n+1}+\boldsymbol{\psi}_m^n\right)=\left[\frac{1}{2}\frac{\partial^2\boldsymbol{\psi}}{\partial z^2}+\frac{k}{4}\frac{\partial^3\boldsymbol{\psi}}{\partial z^2\partial t}+\frac{h^2}{24}\frac{\partial^4\boldsymbol{\psi}}{\partial z^4}+\frac{kh^2}{48}\frac{\partial^5\boldsymbol{\psi}}{\partial z^4\partial t}+\frac{k^2}{8}\frac{\partial^4\boldsymbol{\psi}}{\partial z^2\partial t^2}+O\left(k^2h^2+k^3\right)\right]_m^n \tag{43}$$

$$g\left(\frac{\psi_m^{n+1}+\psi_m^n}{2}\right)=\boldsymbol{g}\left(\boldsymbol{\psi}_m^n\right)+\frac{k}{2}\frac{\partial\mathbf{g}\left(\boldsymbol{\psi}_m^i\right)}{\partial t}+\frac{k^2}{4}\frac{\partial^2\mathbf{g}\left(\boldsymbol{\psi}_m^n\right)}{\partial t^2}+O\left(k^3\right) \tag{44}$$

Now substituting Equations (42) - (44) into Equation (38) gives:

$$\begin{aligned}T_m^n=&\left[\frac{\partial\psi}{\partial t}-\frac{\beta_2}{2}A\frac{\partial^2\psi}{\partial z^2}+\gamma g(\psi)\right]_m^n+\frac{k}{2}\frac{\partial}{\partial t}\left[\frac{\partial\psi}{\partial t}-\frac{\beta_2}{2}A\frac{\partial^2\psi}{\partial z^2}+\gamma_g(\psi)\right]_m^n\\ &+\left[\frac{k^2}{3!}\frac{\partial^3\psi}{\partial t^3}-\beta_2A\left(\frac{h^2}{24}\frac{\partial^2\psi}{\partial z^4}+\frac{kh^2}{48}\frac{\partial^5\psi}{\partial t\partial z^4}+\frac{k^2}{8}\frac{\partial^4\psi}{\partial z^2\partial t^2}\right)+\gamma\frac{\partial^2g(\psi)}{\partial t^2}\right]_m^n+O\left(K^2h^2+k^3+h^4\right),\end{aligned} \tag{45}$$

where T_m^n represents the truncation error.

Since ψ is the exact solution vector of (1) then from (10), the first two brackets equals zero. Thus the truncation error becomes:

$$T_m^n = O\left(K^2 + kh^2 + h^2\right) \tag{46}$$

Proving that the method used is second order in space and time and Crank–Nicolson method is naturally unconditionally stable.

V. EFFECTS OF NONLINEARITY AND DISPERSION IN THE NLSE

Since the optical fiber communication systems first generation were discovered early in the 80's, fiber optic technology has significantly expanded [15]. in order to satisfy the needs of network users, these developments were done. which extends the length of the transmission channel and increases transmission capacity especially for high bit rate communications like real-time image transmission, video conferencing etc [13]. The NLSE shows that the two main phenomenons that affects the fiber optic communication systems are nonlinearity and dispersion and they distort the input pulse signal through the transmission system [12]. It also shows that the dispersion effect and nonlinear effect are closely related.

the medium response when an electromagnetic wave interacts with the bound electrons of a dielectric, depends generally on the optical frequency ω. A property, termed as chromatic dispersion, is manifested via the frequency dependence of the refractive index $n(\omega)$ [11]

In short optical pulse propagation, fiber dispersion performs an important duty, as it is dangerous for optical communication systems to have different spectral components associated with the pulse broadening. Mathematically, by expanding the mode-propagation coeffcient β in a Taylor series about the frequency ω_0 at which the pulse spectrum is centred, fiber dispersion effects are accounted for.

$$\beta(\omega) \doteqdot n(\omega)\frac{\omega}{c} = \beta_0 + \beta_1\left(\omega - \omega_0\right) + \frac{1}{2}\beta_2\left(\omega - \omega_0\right)^2 + \cdots,$$

where c is the speed of light and

$$\beta_m = \left(\frac{d^m\beta}{d\omega^m}\right)_{\omega=\omega_0} \qquad (m = 0, 1, 2, \cdots)$$

Parameters β_1 and β_2 has a relation to the refractive index n and its derivative via the relations

$$\beta_1 = \frac{1}{v_g} = \frac{n_g}{c} = \frac{1}{c}\left(n + \omega\frac{dn}{d\omega}\right), \quad \beta_2 = \frac{1}{c}\left(2\frac{dn}{d\omega} + \omega\frac{d^2n}{d\omega^2}\right),$$

where v_g represents group velocity and n_g represents group index. Since different spectral components of the pulse do not simultaneously reach the fiber output, then the group velocity frequency dependence leads to pulse broadening. Consider an optical fiber of length L; a particular spectral component at the frequency ω would reach at the output end of the fiber at a time delay of $T = L/v_g$: the extent of pulse broadening is governed by the equation below if the spectral width of the pulse is $\Delta\omega$.

$$\Delta T = \frac{dT}{d\omega}\Delta\omega = \frac{d}{d\omega}\left(\frac{L}{v_g}\right)\Delta\omega = L\frac{d}{d\omega}\left(\frac{d\beta}{d\omega}\right)\Delta\omega = \frac{d^2\beta}{d\omega^2}\Delta\omega \equiv L\beta_2\Delta\omega$$

Such a phenomenon is referred to as the group-velocity dispersion (GVD), and β_2 is its parameter. from this it follows that the physical dimension of β_2 is $L^{-1}T^2$. Depending on the sign of β_2 qualitatively different behaviors can be manifested by the nonlinear effects in optical fiber. β_2 disappear at a wavelength of about $1270nm$ in standard silica fibers and becomes negative for longer wavelength, such a wavelength is termed as the zero-dispersion wavelength and represented as γ_D. As $\beta_2 > 0$ at a wavelength $\gamma < \gamma_D$ The fiber exhibits normal dispersion. Low-frequency components of optical pulse travel faster than high frequency components of the same pulse in the normal-dispersion regime. By contrast, in the anomalous-dispersion regime in which $\beta_2 < 0$, the opposite occurs. When the light wavelength goes beyond γ_D, silica fibers exhibit anomalous dispersion. For the study of nonlinear effects the anomalous dispersion regime is of considerable interest as it is in this regime that optical fibers accommodates solitons via a balance between the nonlinear and dispersive effects.

VI. RESULTS AND ANALYSIS

In order to justify the conservation of the quantities hamiltonian, momentum and energy associated to the propagation of pulses, we solve equation (1) using the reduced basis method. The numerical study focuses on the solution of the first-order soliton propagation problem in a single-mode fiber. Computations were done on a personal computer with the following specifications (HP ProBook 450 G7 Intel Core i5-10210U 10th Gen, 500GB HDD and 8GB RAM). In this paper, we discretized the NLSE by the Crank–Nicolson method to obtain the FOM and we implemented the numerical computations in MATLAB, version R2021a.

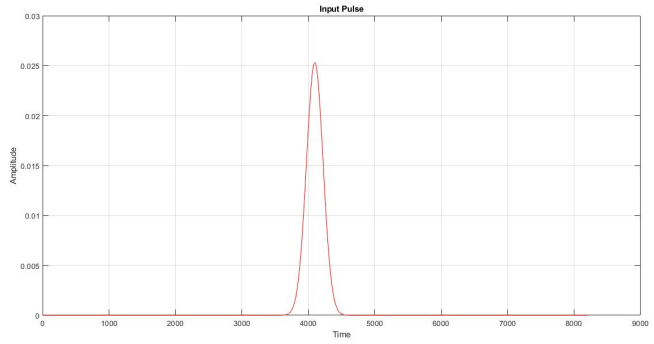

Figure 1: ***Input Pulse***

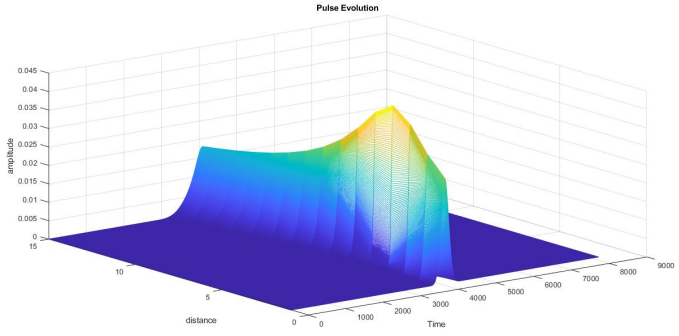

Figure 2: ***Pulse Evolution***

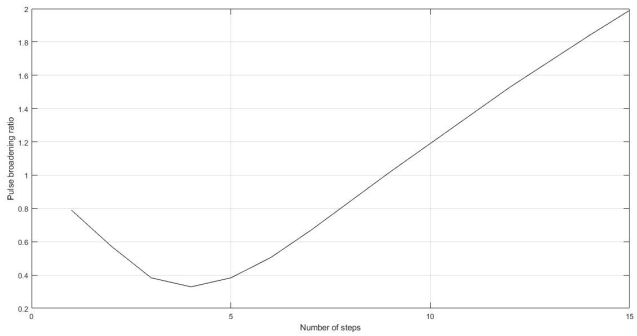

Figure 3: ***Pulse Broadening Ratio***

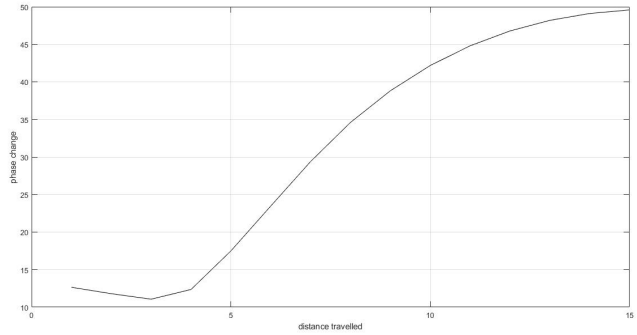

Figure 4: ***Phase Change with Distance Comparision***

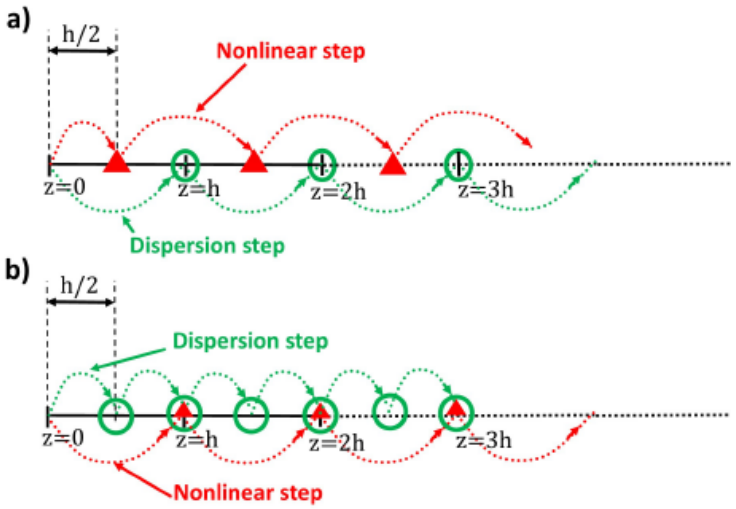

Figure 5: ***Iterative integration over z-propagation for (a) the SSFM and (b) the S-SSFM.***

The pulse input and evolution are presented in Figures 1 and 2 respectively, while Figure 3 represents the pulse broadening ratio with respect to step size, and we noticed that the ratio tends to decrease at small step size (< 5) and tend to increase as the step size increases from 5. Figure 4 represents the phase change with respect to distance travelled and in Figure 5 we illustrate how the SSFM and S-SSFM operates over different subdivisions of the spartial iterative steps. The SSFM is executed over two subgroups of h, the consider the

dispersion contribution to integrate the NLSE in the frequency domain in the first subgroup, then we integrate the nonlinear part in the temporal domain in the second subgroup. In contrast, the S-SSFM operates over three subgroups, in the first and third subgroups we integrate the dispersion contribution and in the second subgroup we integrate the nonlinear part.

Table 1: ***SSFM***

h-step size (m)	**Hamiltonian**	**Momentum**	**Energy**	**Comp. time (s)**
0.005	2.1×10^{-10}	5.9×10^{-12}	7.1×10^{-11}	249.7
1	1.7×10^{-7}	2.9×10^{-14}	4.3×10^{-13}	1.5
5	3×10^{-3}	5.7×10^{-15}	4.9×10^{-14}	0.3
10	1.7×10^{-5}	2.7×10^{-15}	4.4×10^{-14}	0.15
20	6.9×10^{-5}	1.2×10^{-15}	1.8×10^{-14}	0.08

Table 2: ***S-SSFM***

h-step size (m)	**Hamiltonian**	**Momentum**	**Energy**	**Comp. time (s)**
0.005	4.8×10^{-10}	1.2×10^{-11}	1.6×10^{-10}	410
1	3×10^{-11}	5.9×10^{-14}	6.8×10^{-13}	2.2
5	8.1×10^{-11}	1.2×10^{-14}	1.5×10^{-13}	0.45
10	3.5×10^{-9}	6.2×10^{-15}	4.9×10^{-14}	0.23
20	1.7×10^{-8}	2.9×10^{-15}	4.5×10^{-14}	0.12

Table 3: ***RK4IP***

h-step size (m)	**Hamiltonian**	**Momentum**	**Energy**	**Comp. time (s)**
0.005	5×10^{-10}	1.2×10^{-11}	1.6×10^{-10}	1350
1	2×10^{-12}	5.6×10^{-14}	6.7×10^{-13}	6.6
5	8.4×10^{-13}	1.3×10^{-14}	2.9×10^{-13}	1.3
10	1.3×10^{-11}	6.3×10^{-15}	4.5×10^{-12}	0.65
20	4.2×10^{-10}	3×10^{-15}	1.4×10^{-10}	0.34

Table 4: ***RBM***

h-step size (m)	**Hamiltonian**	**Momentum**	**Energy**	**Comp. time (s)**
0.005	4.6×10^{-10}	1.3×10^{-11}	1.5×10^{-10}	255
1	1.8×10^{-12}	5.7×10^{-14}	6.5×10^{-13}	1.8
5	8.1×10^{-13}	1.5×10^{-14}	2.7×10^{-13}	0.4
10	1.8×10^{-12}	6.6×10^{-15}	4.8×10^{-14}	0.18
20	4.9×10^{-11}	3.2×10^{-15}	4.1×10^{-14}	0.10

Tables 1-4 Shows a comparative table of the errors associated to the conservative quantities: Hamiltonian, Momentum and Energy and the computational time of the first-order soliton propagation for a couple of h-step size values using the SSFM, the S-SSFM, the RK4IP and the RBM methods respectively.

As h-step size increases the individual contribution of the round-off error tends to decrease [4]. From this argument, we can decipher that in the cases of (SSFM, S-SSFM, RK4IP and RBM) momentum and energy presents a negligible truncation error ($< 10^{-8}$), so that the the round-off error dominates the total error, which as the h-step size increases tends to decrease. Also, in the case of RK4IP method the energy error for step size $h > 5$ shows that the contribution of the round-off error became amaller than the truncation error; as a result when the h-step size increases the error also increases.

Additionally, Hamiltonian is reproduced properly over the whole h-step size domain by the RK4IP, the RBM and the S-SSFM methods; On the contrary, Hamiltonian in the SSFM only yields a negligible error level for a small h-step size of $h < 1$, as shown in Table 1. Also, Hamiltonian only yields a negligible fluctuation in its error trace for small h-step sizes ($h < 1$) in the case of the S-SSFM and ($h < 5$) in the cases of RK4IP and RBM, showing a round-off error contribution; the numerical methods introduce their typical truncation error contribution for larger h-step size values, which tends to increase as the h-step size increases. On the contrary, the SSFM provides a Hamiltonian error trace driven by the truncation error over the whole h-step size domain.

Finally, order of accuracy and computational time of the methods, from the above tables shows that the RBM and the RK4IP methods has a higher order of accuracy whereas the SSFM and RBM has the least computational time.

VII. CONCLUSION

We studied the pulse propagation in fiber optics formalism modelled by the Nonlinear Schrodinger Equation, in the presence of nonlinearity and dispersion. We solved the NLSE by the reduced basis method (RBM) and the numerical results shows that the properties Hamiltonian, Momentum and Energy are conservative. We compare our solution with several other numerical approaches that had been used in the past to solve the NLSE like S-SSFM, RK4IP and SSFM methods, we came with the conclusion that compared to these three methods the RBM has a higher order of accuracy and after the SSFM it has the least computational time compared to S-SSFM and RK4IP methods.

REFERENCES

[1] A. A. Alanazi, S. Z. Alamri, S. Shafie, S. B. M. Puzi. Solving nonlinear schrodinger equation using stable implicit finite difference method in single-mode optical fibers. wileyonlinelibrary.com/journal/mma, (2021).

[2] Agrawal, G. Nonlinear fier optics (fifth edition). Optics and Photonics, Academic Press, (2013)

[3] Agrawal, G. Nonlinear fiber optics (6th ed). New York: Academic Press, (2019)

[4] Ames, W. F. Nonlinear partial differential equations in engineering vol 18. (New York: Academic Press), (1965)

[5] Christian H. and Hendry D. P. Deep learning of the nonlinear schrodinger equation in fiber-optic communications. CoRR, (2018).

[6] Domenico F. A study of a nonlinear schrodinger equation for optical fibers. UNIVERSITA DEGLI STUDI DI FIRENZE, (2016).

[7] FEDERICO N. et al. Reduced basis method for parametrized elliptic optimal control problems. Society for Industrial and Applied Mathematics, 35 (5), A2316-A2340, (2013).

[8] Jeff H. Understanding fiber optics. LaserLight Press, (2006).

[9] Jens L. E. Reduced basis methods for parametrized partial differential equations. Norwegian University of Science and Technology, (2011).

[10] John C. Introduction to fiber optics. Newnes, (2001).

[11] Muhamad A. and Anak A. S. P. M. Analysis of high order dispersion and nonlinear effects in fiber optic transmission with nonlinear schrodinger equation model. International Conference on Quality in Research, (2015).

[12] P.Agrawal G. Nonlinear fiber optics 3rd edition. California, USA : Academic Press, (1995).

[13] P.Agrawal G. Fiber-optic communication systems. NY: John Wiley, Inc. USA, (2002).

[14] Rozza G. et al. Reduced basis approximation and a posteriori error estimation for affinely parametrized elliptic coercive partial differential equations: application to transport and continuum mechanics. Archives of Computational Methods in Engineering, 15(3):229275, (2008).

[15] Xu, Bo. Study of fiber nonlinear effects on fiber optic communnication system. A P.hD Dissertation, University of Virginia. (2003).